IJCRT.ORG ISSN : 2320-2882

INTERNATIONAL JOURNAL OF CREATIVE RESEARCH THOUGHTS (IJCRT)

An International Open Access, Peer-reviewed, Refereed Journal

ANALYSIS OF MELTING BEHAVIOUR OF IONIC SOLIDS AT HIGH PRESSURES

Rohita Singh* and M. P. Singh
Department of Physics, Institute of Basic Science
Dr. Bhimrao Ambedkar University, Khandari Campus, Agra-282002 (U.P.), India

Abstract : In the present study we have used the volume dependence Grüneisen parameter in the Lindemann law to predict melting curves for ionic solids viz. NaCl and MgO. We have adopted third order Birch-Murnaghan equation of state (EOS) to compute the results for pressure-volume relationship, bulk modulus and its pressure derivatives up to phase transition pressure. The results for melting curves of different solids in the present study using $\gamma_\infty = 1/2$ at extreme compressions are found to be in good agreement with available experimental data. We have also computed melting slopes at different pressures for NaCl and MgO. It is found that the melting tends to zero in the limit of infinite pressure. The obtained results are also found to compare well with the experimental data and molecular dynamics simulations.

Keywords : Grüneisen parameter, Birch-Murnaghan EOS, bulk modulus, melting curves, melting slope.

INTRODUCTION

Equations of state (EOS) describing pressure-volume (P-V) relationships, bulk modulus (K), and its pressure derivative (K'=dK/dP) must satisfy the infinite pressure limit according to which $K'_\infty = 5/3$ [1-3]. In addition, the formulations for the volume dependence of Grüneisen parameter γ must extrapolate to $\gamma_\infty = 1/2$ [4,5] in the limit of infinite pressure or extreme compression $(V \to 0)$. However, various attemps made recently for predicting melting curves of solids [6-12] do not satisfy these constraints. In the present study we formulate an expression for predicting melting temperatures (T_m) of ionic solids viz. NaCl and MgO at high pressures. We use the Jeanloz equation for the volume dependence of gamma [13] by imposing the constraint $\gamma_\infty = 1/2$ which has been firmly established [4, 5]. Values of T_m determined from the Lindemann law [14, 15] at different volume compressions (V/V_0) are transformed to T_m as a function of pressure using the third order Birch-Murnaghan EOS $(K'_\infty = 5/3)$. Melting slopes for different compounds are calculated using values of Grüneisen parameter and bulk modulus at different pressures in the Lindemann law.

ANALYSIS OF COMPUTATIONAL METHOD

According to the Lindemann law of melting [14, 15], we can write

$$\frac{d\ln T_m}{d\ln V} = -2\left(\gamma - \frac{1}{3}\right) \qquad (1)$$

In order to integrate Eq. (1) with respect to volume V we need to know the volume dependence of the Grüneisen parameter γ. Jeanloz [13] obtained the following formula

$$\gamma = \gamma_0 \exp\left[-\frac{q_0}{\lambda}\left\{1-\left(\frac{V}{V_0}\right)^{\lambda}\right\}\right] \qquad (2)$$

where γ_0 is the value of γ at zero-pressure ($V=V_0$). Equation (2) has been derived using the volume dependence of q, the second order Grüneisen parameter

$$\frac{q}{q_0} = \left(\frac{V}{V_0}\right)^{\lambda} \quad (3)$$

in the following relationship [1]

$$q = \frac{d\ln\gamma}{d\ln V} \quad (4)$$

The parameter λ is taken to remain constant with the change in volume for a given material. Equations (3) and (4) taking together, and then integrating with respect to volume we get the Jeanloz equation (2). In the limit of extreme compression $(V \to 0)$, γ tends to γ_∞, a positive finite minimum value, and q tends to zero. These thermodynamic constraints are satisfied by the Jeanloz equations (2) and (3). In the limit $V/V_0 \to 0$, Eq. (2) gives

$$\gamma_\infty = \gamma_0 \exp\left(-\frac{q_0}{\lambda}\right) \quad (5)$$

For an ionic lattice, $\gamma_\infty = 1/2$ has been firmly established [4, 5]. Indeed, in the limit of infinite pressure, melting temperature T_m behaves like $\rho^{1/3}$ or $V^{-1/3}$ where ρ is density. According to the theory of the melting of one-component plasma (OCP) which represents an ionic lattice surrounded by a gas of free electrons making the system electrically neutral. OCP is the limiting state of compressing a solid as pressure becomes infinitely large. According to the theory of melting of OCP, we have

$$\frac{d\ln T_m}{d\ln V} = -\frac{1}{3} \quad (6)$$

Taking $\gamma = \gamma_\infty$, Eq (1) becomes compatible with Eq. (6) only when $\gamma_\infty = 1/2$. Equations (2) and (5) taken together yield

$$\gamma = \gamma_\infty \exp\left[\frac{q_0}{\lambda}\left(\frac{V}{V_0}\right)^{\lambda}\right] \quad (7)$$

When we substitute Eq. (7) for γ in Eq. (1), we get an expression which can not be integrated analytically. In place of Eq. (7) we therefore use the following expression obtained by expanding the right hand side of Eq. (7) upto third order

$$\gamma = \gamma_\infty\left[1 + \frac{q_0}{\lambda}\left(\frac{V}{V_0}\right)^{\lambda} + \frac{q_0^2}{2\lambda^2}\left(\frac{V}{V_0}\right)^{2\lambda} + \frac{q_0^3}{6\lambda^3}\left(\frac{V}{V_0}\right)^{3\lambda}\right] \quad (8)$$

At zero-pressure, $V = V_0$, Eq. (8) yields

$$\gamma_0 = \gamma_\infty\left[1 + \frac{q_0}{\lambda} + \frac{q_0^2}{2\lambda^2} + \frac{q_0^3}{6\lambda^3}\right] \quad (9)$$

Anderson has found [16] that $q_0 = 1$ is a good approximation for many ionic solids and geophysical minerals [17, 18]. Value of λ is then determined with the help of Eq. (9) taking $\gamma_\infty = 1/2$, and γ_0 from Table 1. The results for λ alongwith input data [6, 16-21] are given in Table 1 for NaCl and MgO. Values of Grüneisen parameter γ versus volume compression V/V_0 determined from Eq. (8) are plotted in Figure-1. Substituting gamma from Eq. (8) in the Lindemann law (Eq. 1), and then integrating we find

$$\frac{T_m}{T_{m_0}} = \left(\frac{V}{V_0}\right)^{-2(\gamma_\infty - 1/3)} \exp\left[2\gamma_\infty Q\right] \quad (10)$$

where T_{m_0} is the melting temperature of the material at zero-pressure, and

$$Q = \frac{q_0}{\lambda^2}\left[1-\left(\frac{V}{V_0}\right)^{\lambda}\right] + \frac{q_0^2}{4\lambda^3}\left[1-\left(\frac{V}{V_0}\right)^{2\lambda}\right] + \frac{q_0^3}{18\lambda^4}\left[1-\left(\frac{V}{V_0}\right)^{3\lambda}\right] \quad (11)$$

Values of melting temperature T_m for the compounds at different volume compressions corresponding to high pressures are computed using Eqs. (10) and (11). These are transformed to T_m at high pressures using the results based on the Birch-Murnaghan EOS [22]

$$P = \frac{3}{2}K_0\left(x^{-7} - x^{-5}\right)\left[1 + \frac{3}{4}\left(K_0' - 4\right)\left(x^{-2} - 1\right)\right] \qquad (12)$$

where $x = (V/V_0)^{1/3}$, K_0 is the value of bulk modulus K at P = 0. The expression for bulk modulus, K = –VdP/dV, and pressure derivative of bulk modulus, K' written as follows

$$K = \frac{1}{2}K_0\left(7x^{-7} - 5x^{-5}\right) + \frac{3}{8}K_0\left(K_0' - 4\right)\left(9x^{-9} - 14x^{-7} + 5x^{-5}\right) \qquad (13)$$

$$K' = \frac{K_0}{8K}\left[\left(K_0' - 4\right)\left(81x^{-9} - 98x^{-7} + 25x^{-5}\right) + \frac{4}{3}\left(49x^{-7} - 25x^{-5}\right)\right] \qquad (14)$$

Here K_0' is the pressure derivative of bulk modulus, $K' = dK/dP$ at zero-pressure. The input parameters used in computations are also given in Table 1. The results for P, K and K' obtained with the help of Eqs. (12), (13) and (14) using the EOS parameters (Table 1) are reported in Table 2 for the compounds at different volume compressions.

RESULTS AND DISCUSSION

The melting curves, T_m versus P, are obtained by using Eqs. (10) and (11), and the data given in Tables 1-2. The results for NaCl up to pressures less than 30 GPa are given in Figure 2. Above this pressure range, NaCl is transformed from B_1 (rock salt phase) to B_2 (CsCl) structure. A comparison of the results obtained in the present study for NaCl has been made with the available experimental data [23] and also with those determined from molecular dynamics [24] MD simulation (Figure 2). The melting curves for MgO is given in Figure 3 along with the available experimental data [23, 25] and the values determined from the MD simulation studies [24, 26-28]. For NaCl and MgO, the results obtained in the present study are closer to the experimental data [23, 25] than those based on the MD simulations. The experimental data reported by Zerr and Boehler [25] give a nearly flat melting curve for MgO which has been challenged by several authors [10]. However, the present work on MgO is consistent with the results obtained by Zerr and Boehler. Okamoto and Fuchizaki [29] have used a one-phase approach based on the earlier formulations [30, 31] for predicting melting curve of MgO. They extrapolated melting temperatures at high pressures up to 200 GPa [29] using the available experimental data for MgO [25]. The micro-texture analysis was performed by Kimura et al [32] to determine melting temperatures of MgO at high pressures which turned out to be much higher than those determined using laser-heated diamond anvil cell. The values of T_m for MgO at CMB pressure determined from micro-texture analysis is nearly 7900K [32]. The corresponding value obtained in the present study for MgO at CMB pressure is closer to 6000K determined [29] by extrapolating the experimental data [25].

Boehler et al [23] reported the experimental melting data also for NaCl. In Figure 2 we have compared the experimental values [23] with those calculated in the present study for NaCl with the help of Eq. (10) taking $\gamma_\infty = 1/2$ and the third order Birch-Murnaghan EOS results in the Lindemann law of melting. The results for melting temperature are found to compare well with the available experimental data (Figure 2). It should be mentioned that there is a similarity between NaCl and MgO. Both the materials are composed of ions (Na^+, Cl-) and (Mg^{2+}, O^{2-}) which are isoelectronic with each other having same number of electrons. However, the nature of chemical bond in MgO is more covalent than that of NaCl which is predominantly ionic [33]. A precisely quantitative analysis of the fractional ionic and covalent character for a large number of binary compounds has been presented by Phillips [34]. According to the Phillips ionicity-covalency model MgO is significantly more covalent than NaCl. This is responsible for the higher value of T_m in case of MgO.

We have also determined slopes of melting curves for different solids at zero-pressure and at high pressure using the following formula [14-16]

$$\frac{d\ln T_m}{dP} = \frac{2\left(\gamma - \frac{1}{3}\right)}{K} \qquad (15)$$

Values of γ determined from Eq. (8) given in figure 1 for NaCl and MgO and bulk modulus K from Eq. (13) are substituted in Eq. (15) to find $d\ln T_m/dP$ at different pressures. Values of slopes computed from Eq. (15) at different pressures are given in table 3 and plotted in Figures 4-5. The plots given in figures

4-5 reveal that values of d $\ln T_m/dP$ decrease with increase in pressure, and tend to zero in the limit of infinite pressure. This is consistent with the earlier predictions made about the variations of melting slopes with the increase in pressure [35-38].

CONCLUSIONS

Burakovsky and Preston [4] developed a theory of melting for elemental solids including metals by using two important thermodynamic constraints viz. $\gamma_\infty = 1/2$ and $K'_\infty = 5/3$. In the present study we have investigated melting curves and their slopes for ionic solids viz. NaCl, MgO using the Burakovsky-Preson thermodynamic constraints in the Jeanloz equation for the volume dependence of Grüneisen parameter with $\gamma_\infty = 1/2$, and the Birch-Murnaghan EOS $(K'_\infty = 5/3)$. The results for melting obtained here with the help of the Lindemann law are found to present close agreement with the available experimental data and the MD simulation results.

TABLE 1 : The input value of K_0, K'_0 and γ_0 at ambient condition [6, 16-21] given in table 1. λ for volume dependence of Grüneisen parameter has been computed from Eq. (9)

Compound	**K_0 (GPa)**	K'_0	γ_0	λ
NaCl	24	5.35	1.60	0.84
MgO	162	4.29	1.54	0.87

TABLE 2 : Results obtained from the third order Birch-Murnaghan EOS. All values of P and K are given in GPa.

$\frac{V}{V_0}$	**NaCl**			**MgO**		
	P	**K**	K'	**P**	**K**	K'
1.0	0	24.0	5.35	0	162	4.29
0.95	1.41	31.2	5.20	9.24	199	4.18
0.90	3.34	40.4	5.07	21.2	245	4.10
0.85	5.98	52.2	4.97	36.8	302	4.05
0.80	9.59	67.4	4.90	57.2	373	4.00
0.75	14.6	87.1	4.84	84.0	462	3.96
0.70	21.4	113	4.80	120	577	3.92
0.65	31.1	148	4.78	168	725	3.89
0.60	44.7	195	4.76	233	921	3.87

TABLE 3 : Values of melting temperatures [23, 25] and melting slopes at ambient pressure, Eq. (15).

	T_{m0} (K)	**$(d\ln T_m/dP)_0$** (GPa^{-1})
MgO	3073	0.015
NaCl	1074	0.104

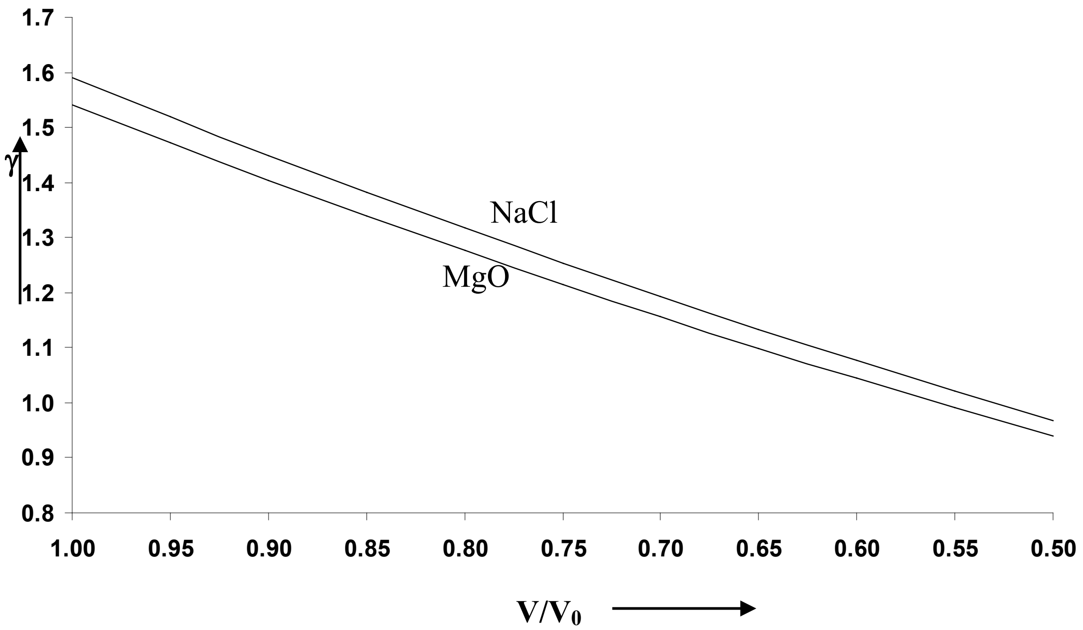

Figure 1 : Plots between the values of Grüneisen parameter (γ) calculated from Eq. (8) and volume compressions (V/V_0) for NaCl and MgO.

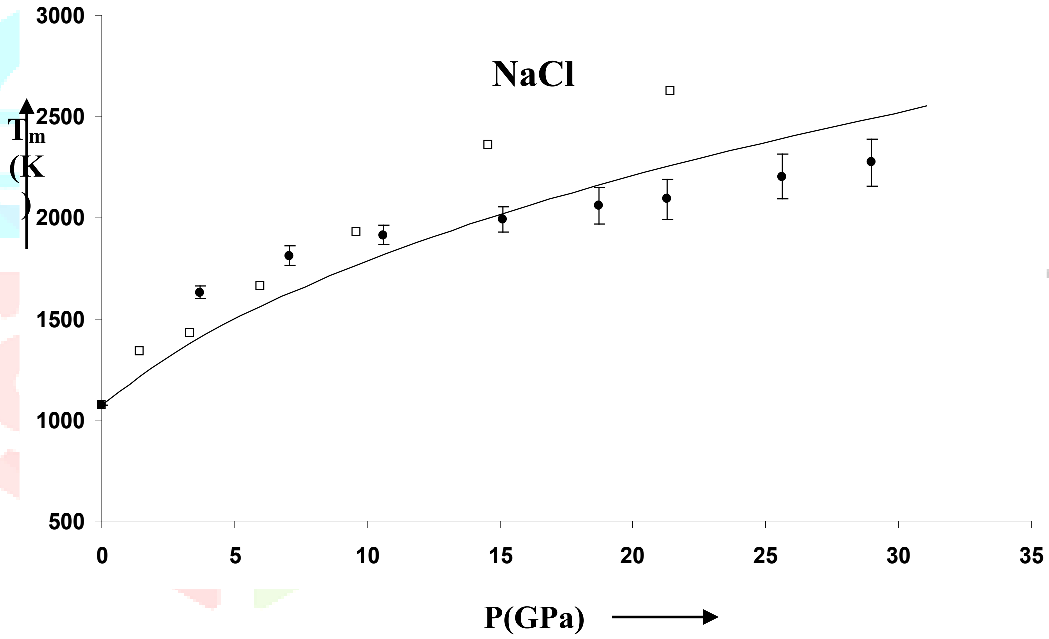

Figure 2 : Plot between melting temperature T_m (K) and pressure P (GPa) for NaCl. Continuous curve (—) represents values calculated by using Eq. (10). Experimental values are shown by symbol **(●)** with error bars [23]. Results based on molecular dynamic simulation [24] are represented by symbol (□).

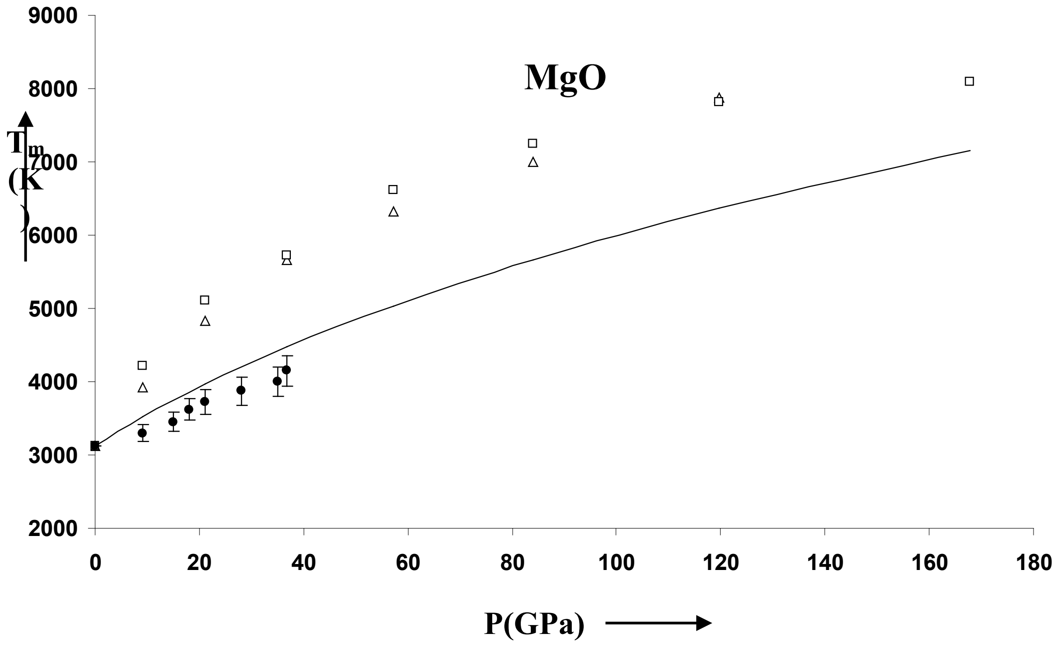

Figure 3 : Plot between melting temperature T_m (K) and pressure P (GPa) for MgO. Continuous curve (—) represents values calculated by using Eq. (10). Experimental values are shown by symbol **(●)** with error bars [25]. Results based on molecular dynamic simulation [26] are represented by symbol (□) and DFT-LDA method [27] represented by symbol (**Δ**).

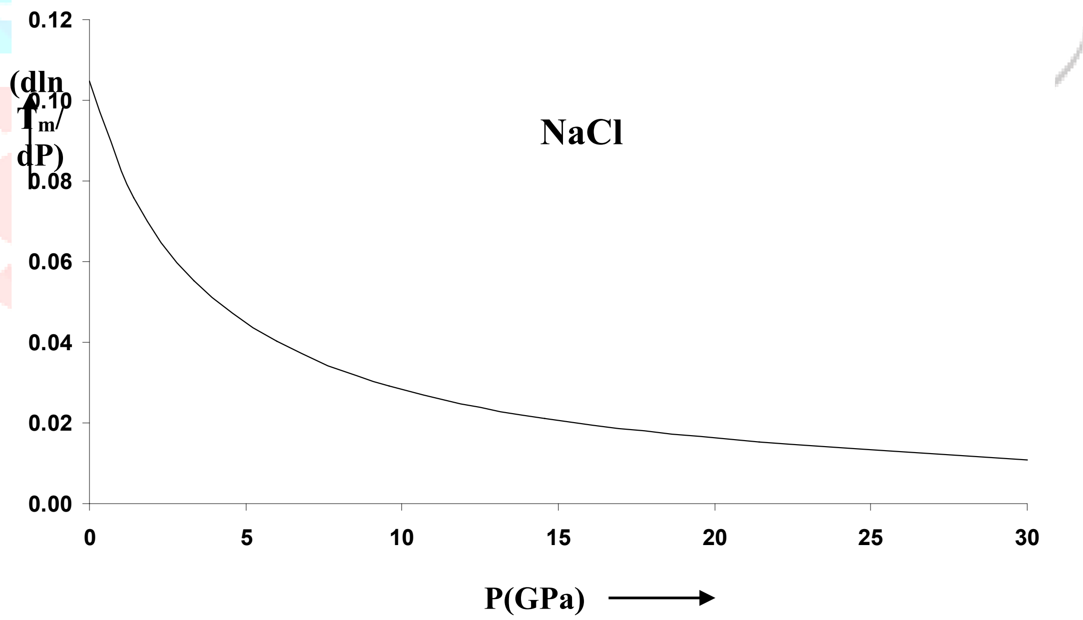

Figure 4 : Plot between values of melting slopes (dln T_m/dP) in GPa^{-1} calculated from Eq. (15) and pressure P (GPa) for NaCl.

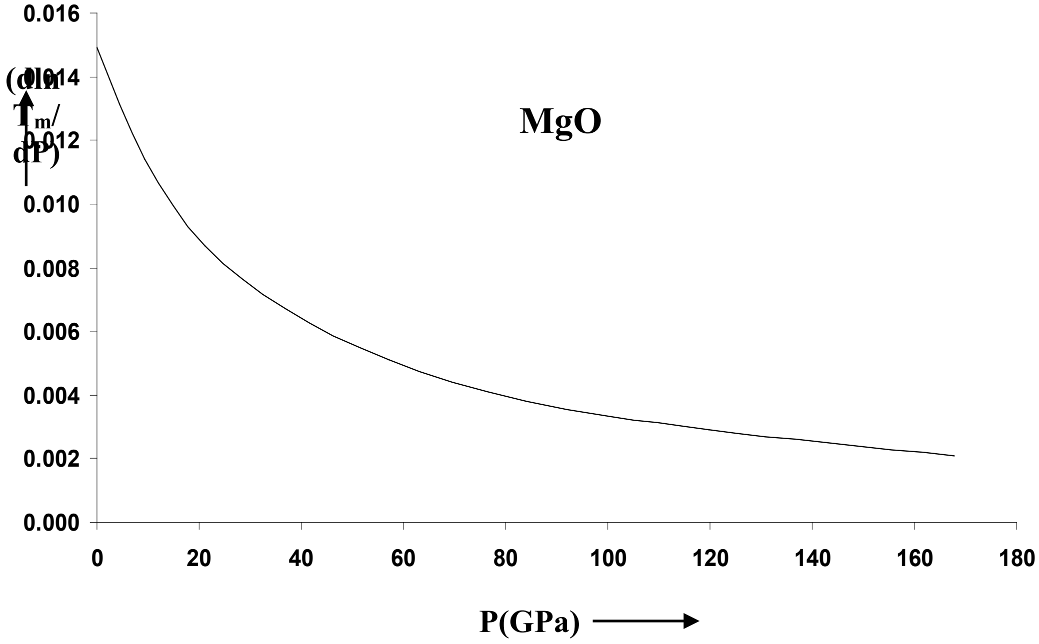

Figure 5 : Plot between values of melting slopes (dln T_m/dP) in GPa^{-1} calculated from Eq. (15) and pressure P (GPa) for MgO.

REFERENCES

[1] W.B. Holzapfel, Physics of solids under strong compression Rep. Prog. Phys. **59** (1996) 29.

[2] W.B. Holzapfel, Equations of state for solids under strong compression, High Press. Res. **16** (1998) 81.

[3] W.B. Holzapfel, Effects of intrinsic anharmonicity in the Mie- Grüneisen equation of state and higher order corrections, High Press. Res. **25** (2005)187.

[4] L. Burakovsky and D.L. Preston, Analytic model of the Grüneisen parameter at all densities, J. Phys. Chem. Solids **65**, (2004) 1581.

[5] J. Shanker, B.P. Singh and H.K. Baghel, Volume dependence of the Grüneisen parameter and maximum compression limit for iron, Physica B, 387 (2007) 409 .

[6] K. Sunil, S.B. Sharma and B.S. Sharma, Analysis of melting curves of MgO and LiF using the Lindemann law, Int. J. Mod. Phys. B **30**, (2018) 1850339.

[7] M. Goyal, Melting temperature of metals under pressure Chinese J. of Phys. **66** (2020) 453.

[8] K. Sunil, D. Ashwini and V.S. Sharma, Pressure dependence of the Grüneisen parameter and melting temperature of some metals, Int. J. Mod. Phys. B. **35**, (2021) 2150255.

[9] D. Ashwini, V.S. Sharma and K. Sunil, Analysis of melting of some metals using pressure dependence of the Grüneisen parameter in the Lindemann law, Eur. Physical J. Plus **137**, (2022) 1.

[10] K. Anand, K. Rajesh and V.S. Sharma, Melting curves of diatomic solids using the Lindemann law and a density-dependent Grüneisen parameter, Comp. Cond. Matter **30**, (2022) e00647.

[11] P. Singh, B.K. Pandey, S. Mishra and A.P. Srivastava, Formulation for the prediction of melting temperature of metallic solids using suitable equation of states, Comp. Cond. Matter **35**, (2023) e00807.

[12] K. Sunil, M.P. Singh and B.S. Sharma, Analysis of melting behaviour of some transition metals at high pressures, Comp. Cond. Matter **35**, (2023) e00813.

[13] R. Jeanloz , Shock Wave Equation of State and Finite Strain Theory, J. Geophys. Res. **94**, (1989) 5873.

[14] F.A. Lindemann, About the calculation of molecular own frequencies, Z. Phys. **11**, (1910) 609.

[15] J.J. Gilvarry, The Lindemann and Grüneisen laws, Phys. Rev. **102**, (1956) 308.

[16] O.L. Anderson, Equation state of solids in geophysics and ceramic science, Oxford University Press Inc. New York (1995).

[17] F.D. Stacey and P.M. Davis, High pressure equation of state with applications, Phys. Earth Planet. Inter. **142**, (2004) 137.

[18] J. Shanker, K. Sunil and B.S. Sharma, The Grüneisen parameter and its higher order derivatives for the Earth lower mantle and core, Phys. Earth Planet. Int. **262**, (2017) 41.

[19] K. Sheelendra and A. Vijay, Equation of state, thermoelastic properties and melting behaviour of NaCl at high temperatures and high pressures, J. Phys. Chem. Solids, **123**, (2018) 364.

[20] K. Sunil, K. Anand and B. S. Sharma, Pressure dependence of melting temperatures for alkali halides, Indian J. Pure Appl. Phys. **51** (2013) 444.

[21] S.S. Kushwah, N.K. Bharadwaj, Analysis based on equation of state for sodium halides, J. Phys. Chem. Solids **70**, (2009) 700.

[22] F. Birch, J. Geophys. Res. **91** (1986) 4949.

[23] R. Boehler, M. Ross and D. B. Boercker, Melting of LiF and NaCl at 1 Mbar : Systematics of ionic solids at extreme conditions , Phys. Rev. Lett. **78**, (1997) 4589.

[24] A.B. Belonoshko, L.S. Dubrovinsky, Molecular dynamics of NaCl (B1 and B2) and MgO (B1) melting; two-phase simulation, American Mineral. 81, (1996) 303.

[25] A. Zerr and R. Boehler, Constraints on the melting temperature of the lower mantle from high-pressure experiments on MgO and magnesioüstite, Nature (London) **371**, (1994) 506.

[26] L. Vocadlo and G.D. Price, The melting of MgO — computer calculations via molecular dynamics, Phys. Chem. Miner. **23**, (1996) 42.

[27] D. Alfe, Melting Curve of MgO from First-Principles Simulations, Phys. Rev. Lett. **94**, (2005) 235701

[28] **R. Boehler, M. Ross and D. B. Boercker,** High-pressure melting curves of alkali halides, **Phys. Rev. B 53, (1996) 556.**

[29] K. Okamoto, K. Fuchizaki, A One-Phase Approach for Predicting the Melting Curve of MgO , J. Phys. Soc. Jpn. **86**, (2017) 064602.

[30] M. Kumari, N. Dass, The melting laws, Phys. Status Solidi B **146**, (1988) 105.

[31] V.V. Kechin, Melting curve equations at high pressure**,** Phys. Rev. B **65**, (2001) 052102.

[32] T. Kimura et al., Melting temperatures of MgO under high pressure by micro-texture analysis , Nat. Commun. **8**, (2017) 15735.

[33] L. Pauling, The nature of the chemical bond and the structure of molecules and crystals, Cornell University Press, Ithaca, New York, (1993).

[34] J. C. Phillips, Ionicity of the chemical bond in crystals, Rev. Mod. Phys. **42**, (1970) 317.

[35] K. Ksiazek and T. Gorecki, Regularities in changes of the activation energy for self and impurity diffusion in alkali halides on passing through the melting point, Defect Diffus. Forum **143**, (1997) 1265.

[36] K. Ksiazek and T. Gorecki, Vacancies and a generalised melting curve of alkali halides, High Temperatures- High Pressures **32**, (2000) 185.

[37] K. Kholiya, J. Chandra, A theoretical model to study melting of metals under pressure, Modern Phys. Lett. B **29**, (2015) 1550161.

[38] J. Shanker, K. Anand, B.S. Sharma and A. Vijay, On the applicability of Lindemann's law for the melting of alkali metals, Int. J. Thermophys. **41**, (2020) 1.